Morphology dependence of photocatalytic activity of zinc oxide nanostructures on water disinfection

Sekineh Khodadad[1], Davoud Dorranian[2]* , Peyman Azimi Anaraki[1], Reza Mirnejad[3], Tania Davari Mahabadi[4]

[1]*Physics Department, Takestan Branch, Islamic Azad University, Takestan, Iran.*
[2]*Laser Lab., Plasma Physics Research Center, Science and Research Branch, Islamic Azad University, Tehran, Iran.*
[3]*Molecular Biology Research Center, Baqiyatallah University of Medical Sciences, Tehran, Iran..*
[4]*Department of Physics and Biophysics, Faculty of Health, Tehran Medical Sciences, Islamic Azad University, Tehran, Iran.*

*Corresponding author: doran@srbiau.ac.ir ; d.dorranian@gmail.com

Abstract:

Dependence of the photocatalytic activities of zinc oxide (ZnO) nanostructures on their morphology was investigated experimentally. Spherical and nanorod morphologies of ZnO nanostructures were synthesized by laser ablation and hydrothermal methods respectively, and were characterized by FESEM images and UV-Vis-NIR spectra. The bandgap energy of ZnO nanospheres was 3.75 eV, while for the ZnO nanorods the bandgap energy was 3.07 eV. Their photocatalytic activities to decontaminate water polluted *Escherichia coli (E. coli)* bacteria were examined in the dark condition and under the UV irradiation. Furthermore, effects of other parameters including size, illumination power, and time were observed. The ZnO nanorods exhibited higher inactivation efficiency in comparison with spherical nanostructures. Results show that in the decontamination process, after distraction of the membrane of *E. coli*, the intercellular dissolved matters including proteins, and sugars flowed out gradually leaded to complete decay of the cell. Results confirm that the area and bandgap energy of nanostructures have determinative role in their photocatalytic activities.

Keywords: ZnO nanoparticle; Escherichia coli; Photocatalytic activity; Nanorod

1. Introduction

Water pollution is the leading cause of death and disease worldwide. According to the World Health Organization anticipation, in 2030, one in three people will not have access to safe drinking water [1]. The presence of various microorganisms, especially human pathogens in water, causes many health problems for humans. Although the preparation of antimicrobial drugs has played an important role in reducing the pathogenicity and mortality of many infectious diseases, but because of chemical side effects and because bacteria can become resistant to antibiotics, drugs lose their effectiveness. Extensive antibacterial properties at environment temperature and in a short time, cheapness, no production of disinfectant by-products harmful to health during use

and after that, high solubility and non-corrosiveness are the characteristics of a suitable disinfectant [2].

One of the photo-chemical-physical methods with all the mentioned characteristics to split chemical or biological pollutant agents from water is the usage of photocatalysts. The use of photocatalysts in water decontamination has been considered intensively since the manufacture of materials in nanometer dimensions became common. The significant increase in the surface to volume ratio of nanoparticles has led to a significant increase in their photocatalytic performance, which is caused by the absorption of radiant photons [3–6]. The review of the work done in this field shows that the main targets of researchers should be in solving two problems. The first is the use of cheap and common nanomaterials for

this purpose. Although the use of complex nanomaterials may increase the efficiency of the photocatalytic activity, but their production on an industrial scale is a new problem. The second is to synthesize nanomaterials that can have high efficiency under visible light irradiation. It cannot be expected that the use of UV radiation in the photocatalytic method of water decontamination on a large scale can be feasible and cost-effective. This is where the engineering of nanocatalysts becomes important. Changing the morphology, reducing the energy gap, adding elements such as sulfur or nitrogen to them, or alloying them with other materials are among the things that can increase the photocatalytic efficiency of a simple nanoparticle.
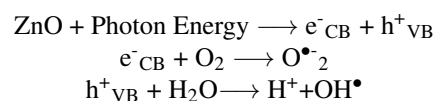
In this experimental research two morphologies of zinc oxide nanoparticles were synthesized, using two different methods of laser ablation and hydrothermal. Properties of both of them were investigated and finally their photocatalytic activities against *Escherichia coli* bacteria in water were observed.

Zinc oxide is widely used semiconductor nanocomposite. It is cheap and easy to produce. It is a white powder that is insoluble in water. ZnO is used as an additive in numerous materials and products including cosmetics, food supplements, rubbers, plastics, ceramics, glass, cement, lubricants, paints, sunscreens, ointments, adhesives, sealants, pigments, foods, batteries, ferrites, fire retardants, and first-aid tapes. It also wide range applications in pharmaceutical and health industries due to its antimicrobial, antiseptic and desiccant properties [7–9].

Apart from the antibacterial photocatalytic property, ZnO itself has shown intrinsic antibacterial properties. The antimicrobial effects of nanometer sized zinc oxide particles can be explained by several mechanisms. The nanoparticles, through close contact with the cell, alter the bacterial microenvironment, eventually damaging the membrane by increasing the solubility of the metal or the production of reactive oxygen radicals. The loss of membrane arrangement is due to accumulation of nanoparticles on the bacterial membrane and penetrating the intracellular contents. Furthermore, induction of oxidative stress due to the production of reactive oxygen radicals from the surface of zinc oxide (reactive oxygen species: ROS), the reaction of these reactive oxygen radicals with DNA, proteins and lipids, leads to cell death. On the other hand, released zinc ions Zn^{+2}, bind to the membranes of microorganisms to exert antimicrobial effects [9–13].

Focus of this work is on the photocatalytic activity of ZnO nanoparticle. Semiconductor oxides can be used as photocatalysts in advanced oxidation processes. They have been exploited as a new and efficient method in contaminated environments. In this method, the electrons in the nano-photocatalyst valance band are excited under ultraviolet light and transferred to the conducting layer by passing through the bandgap. As a result of this excitation, an electron-hole pair is formed which is able to redox a wide range of organic pollutants, bacteria and fungi during a series of redox reactions by producing reactive oxygen O_2^- species and hydroxyl radicals OH. Reactions of photocatalytic mechanisms of ZnO nanoparticles to destruct the bacteria are;

$$ZnO + Photon\ Energy \longrightarrow e^-_{CB} + h^+_{VB}$$
$$e^-_{CB} + O_2 \longrightarrow O^{\bullet-}_2$$
$$h^+_{VB} + H_2O \longrightarrow H^+ + OH^\bullet$$

This mechanism is illustrated in detail in Fig. 1. Although reactive oxygen ions and hydroxyl radicals are the main responsible of photocatalytic mechanisms but role of ZnO NPs is not negligible.

For years, research has been conducted on the properties of zinc oxide nanostructures including its decontamination and photocatalytic properties. Recently, effects of different morphologies of zinc oxide nanostructures has been at the focal points of several researches. Thakur et al. worked on the morphology engineering of ZnO nanorod arrays to hierarchical nanoflowers for enhanced photocatalytic activity and antibacterial action against Escherichia coli. They found that photocatalytic activity of nanorod ZnO is more effective than nanoflower in removing water bacterial contamination [14]. Raj et al. investigated the effects of harnessing ZnO nanoparticles for antimicrobial and photocatalytic activities. They compared the photocatalytic antibacterial efficiencies of rectangular flake like and spherical ZnO nanostructures [15]. In another work Thakur et al. reported about the effects of morphology of ZnO nanostructures for caffeine degradation and Escherichia coli inactivation in water [16].
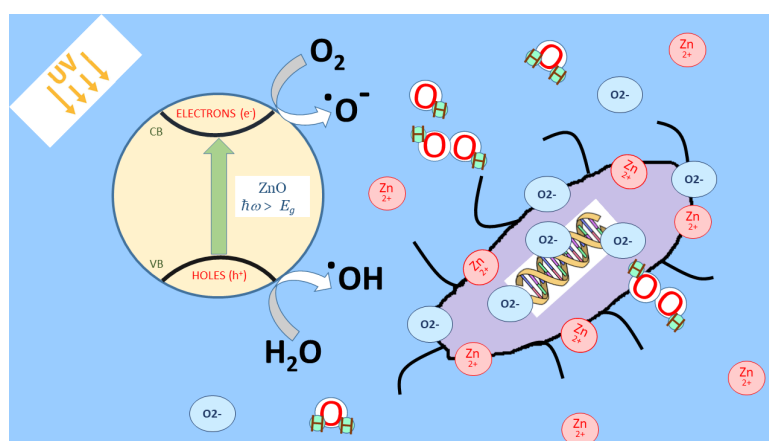

Figure 1. Schematic diagram of photocatalytic mechanisms of ZnO nanoparticles to destruct the bacteria.

Sharma et al. investigated the influence of size and shape of ZnO nanoparticles (hexagonal, spherical, cylindrical and cuboidal shapes) on their antimicrobial photocatalytic efficiency. They found that area of nanoparticles are more effective than their shape [17]. Furthermore, in this field, Sawai studied the effect of oxygen radicals produced by zinc oxide on its antimicrobial effect and found that the production of H_2O_2 during the photocatalytic process enhance the antimicrobial properties[13, 18]. Furthermore, the concentration of hydrogen peroxide increases linearly with the concentration ZnO NPs. According to Naval's experiments, Zn^{+2} and H_2O_2 amounts are small, so the predominant mechanism for disinfection is mainly due to the presence of ZnO. This assumption was in line with Zhang et al. studies [19]. The studies by Jones et al. [20] explored that the photocatalytic properties of zinc oxide are effective. On the other hand, the use of ultraviolet light in the process of water disinfection and wastewater treatment is a well-known method to replace disinfectant chemicals such as chlorine. Ultraviolet light disinfects effectively without the production of harmful side effects from chemical disinfectants such as chlorination [21, 22].

Escherichia coli is an opportunistic bacterium characterized by motility, gram-negative, glucose fermentation and gas production, mannitol positive, sucrose positive, endol positive, methyl red positive, citrate negative, hydrogen sulfide negative. According to the World Health Organization standard, only a zero count of *Escherichia coli* in drinking water is considered to be safe. Therefore, it is necessary to disinfect drinking water from this resistant bacterium or reduce it to the relevant standards.

In this paper, dependence of the photocatalytic activities of zinc oxide (ZnO) nanocomposite on their morphology was investigated experimentally. The disinfection of *Escherichia coli* bacteria in water was carried out in dark condition and under the influence of UV radiation. Results show that although both ZnO morphologies are effective photocatalysts to decontaminate water from bacterial pollutant but the efficiency may be increased by choosing a suitable morphology.

2. Experimental detail

2.1 ZnO nanoparticles production and characterization

Spherical zinc oxide nanoparticles were synthesized by pulsed laser ablation method. Before the experiment Zn plate was polished and all containers as well as Zn target were cleaned in ultrasonic bath of acetone, alcohol, and distilled water respectively for 20 min. To carry out the ablation process, the Zn plate was placed at the bottom of a container filled with 20 ml of distilled water. Height of water on the surface of the target was 5 mm. Ablation was done by 1000 pulses of the fundamental wavelength of a Q-switched Nd:YAG laser at 1064 nm wavelength with the pulse duration of 7 ns, repetition rate of 10 Hz and fluence of 1 J/cm^2. The laser pulse was focused on the surface of target by means of 100 mm focal length lens. Spot size of the laser beam on the surface of the target was calculated to be about 25 μm. Laser source was introduced in our former reports [23–25].

Rod shape zinc oxide nanoparticles were synthesized by hydrothermal method. 0.5 M zinc nitrate solution was prepared in 30 mL distilled water under stirring for 30 min. Meanwhile 5 M sodium hydroxide solution was prepared by mixing NaOH in 30 mL distilled water under stirring for same duration. NaOH solution was added dropwise to zinc nitrate solution under continuous stirring until pH value of the reactants increased to 12. A teflon lined sealed stainless-steel autoclaves was employed to keep this solution mixture in the hydrothermal oven at a temperature of 125 °C for 2h. Then the beaker was taken outside and allowed to cool naturally to room temperature. After the reaction was completed, the resulting white solid products were washed, filtered and then dried in air in a laboratory oven at 60 °C [26, 27]. Morphology and size of both (spherical and rod shape) produced zinc oxide nanoparticles was observed by a Zeiss Sigma-500 system. The optical properties of nanoparticles include their absorption peaks and bandgap energies were studied by the recorded spectra of T80 spectrometer from PG instrument.

2.2 Photocatalytic activity and antibacterial assay

MIC and MBC of both nanomaterials including spherical ZnO and nanorod ZnO nanostructures and imipenem (as control) were evaluated for the clinical isolates of *E. coli* using the standard guidelines of the CLSI. Briefly, an initial bacterial inoculum containing 1.5×108 CFU/mL (0.5 McFarland) of isolates was inoculated in cation-adjusted Mueller-Hinton broth (CAMHB; BD Diagnostic Systems, adjusted to pH = 5.9) in a 96-well microplate. The inoculated wells were exposed to serial micro dilutions of distilled water and imipenem. The endpoints were determined when no turbidity was observed in the well. Then, the microplate was incubated for 24 h at 37 °C. After 24 h of incubation, the absorbance of each well was measured at 600 nm using a microtiter plate reader. The lowest concentrations that inhibited the growth of 50% and 99% of bacteria were considered as MIC and MBC, respectively. Each experiment was repeated three times [28].

For analyzing the post-treatment bacterial viability and determining the minimum time needed for reaching an inhibitory or bactericidal effect, viable *Escherichia coli* bacteria were counted at various concentrations of spherical and nanorod ZnO nanostructures. Results are presented in Fig. 2. The killing time curve was delineated for the survived Escherichia coli isolates post-challenged by both ZnO nanostructures and imipenem at their MIC values (16 mg/μL, 32 mg/μL, respectively). For this purpose, the standard isolate of *Escherichia coli* at the exponential phase of growth was obtained by culturing in Muller–Hinton broth (MHB). A standard 0.5 McFarland suspension (1.5×108 CFU/mL) of each was aliquoted in a microplate and diluted to 5×105 CFU/mL (1/300). The diluted bacteria suspension was mixed with Muller–Hinton broth (MHB) and Muller-Hinton agar (MHA), and imipenem and incubated at 37 °C. Each aliquot was sampled at 0, 0.5, 1, 2, 4, 8, 16, 18, and 24 h, and cultured on Muller-Hinton agar (MHA) for another 24 h at 37 °C. Colony count was exerted after 24 h to obtain the CFU of each aliquot at either 0, 0.5, 1, 2,
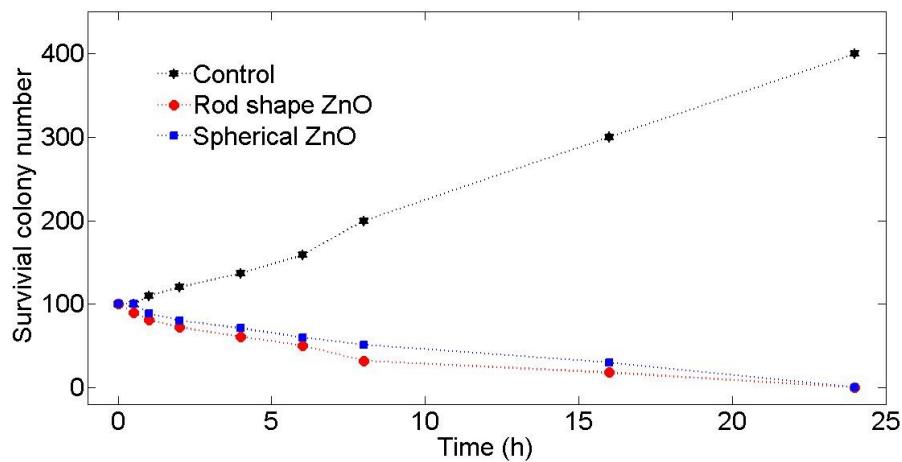
Figure 2. The survival colony number of *E. coli* bacteria under the effects of ZnO nanostructures with different shapes (without UV radiation).

4, 8, 16, 18, or 24 h [29, 30].

The experiments were begun with 100 colonies. Without any nanostructures number of colonies was growth to 400 after 24 hours. But with the presence of ZnO nanostructures all *E. coli* colonies were deactivated in completely. Growth and deactivation processes were almost linearly. The growth rate was larger than deactivation rate. And the deactivation rate for the case of nanorod ZnO nanostructures was slightly larger than for the case of spherical nanostructures. It is due to the larger area of nanorod ZnO nanostructures in comparison with spherical nanoparticles. The contact area between nanostructures and bacteria plays an important role in deactivation process.

3. Results and discussion

3.1 Nanostructures

SEM images of nano sphere and nanorod ZnO nanostructures are presented in Figs. 3a and 3b respectively. ZnO nanoparticles which were synthesized by laser ablation method were spherical with about 20-30 nm diameter. Fig. 3b shows the hydrothermal method produced ZnO nanostructures. Their length was about 200 nm with 30-40 nm width. Figures show that the rate of adhesion is

high for both nanostructures but the density of rod shaped ZnO nanostructures is higher in comparison with ZnO nanospheres.

The UV-Vis-NIR absorption spectra of nanocomposites are depicted in Figs. 4 . Spectra were recorded from the nanocomposites suspensions in 1 cm thickness quartz cells. For the case of spherical ZnO nanoparticles a single peak was occurred in the absorption spectrum at 300 nm due to excitonic oscillations of this semiconductor nanomaterial. The large FWHM of this peak shows that the size of synthesized nanoparticles is not uniform. The absorption spectrum of rod shaped ZnO nanostructures has two peaks at 360 nm and 385 nm. These peaks are due to excitonic oscillation of ZnO nanoparticles along the length and width of nanostructures respectively. The small FWHM of both peaks confirms that their size distribution has smaller width in comparison with ZnO nanoparticles. Different absorption spectra of laser ablation produced nanoparticles and hydrothermal method produced ZnO nano rods is in good agreement with our observation from SEM images [23, 24]. The bandgap energies of both ZnO nanostructures were extracted by using their transmission spectra in the equation
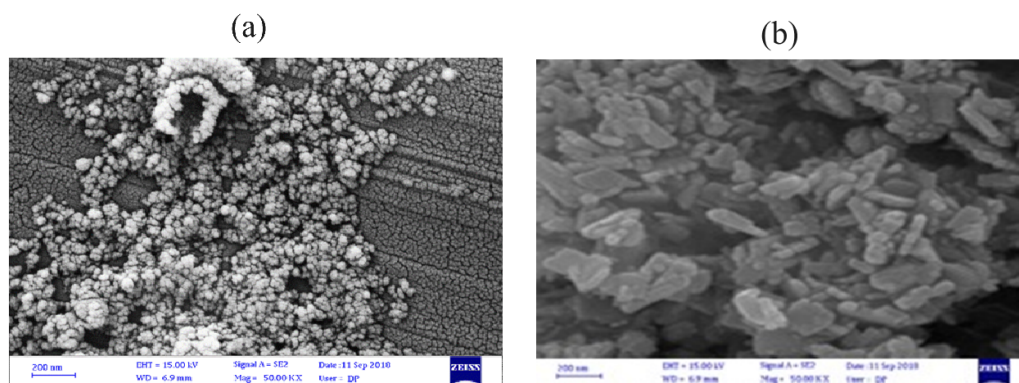
(a)   (b)

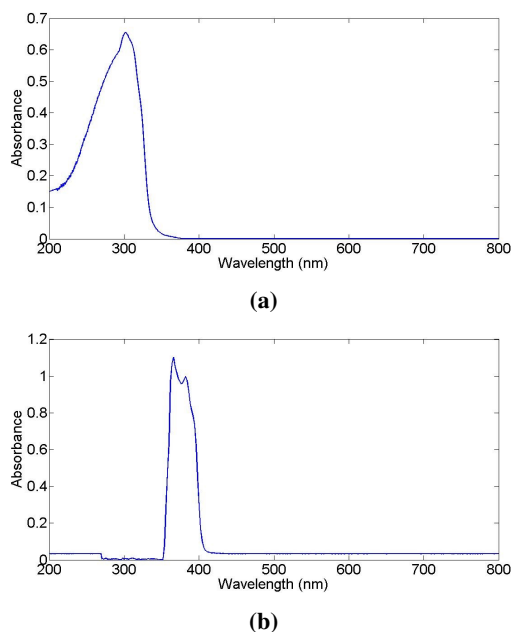**Figure 3.** SEM images of a) spherical and b) nanorod synthesized ZnO nanoparticles.

Figure 4. UV-Vis-NIR absorption spectra of a) spherical and b) nanorod ZnO nanostructures.
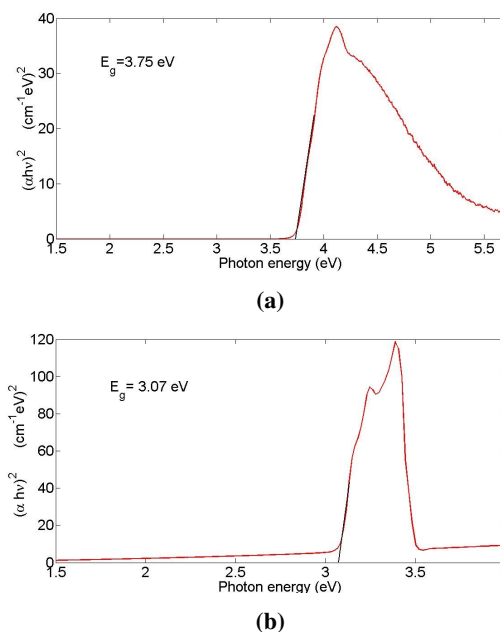

Figure 5. Tauc plots to extract the bandgap energy of a) spherical and b) nanorod ZnO nanoparticles due to their allowed direct transitions.

of Tauc law [31].

$$(\alpha h\nu) = A(h\nu - E_g)^m \tag{1}$$

This equation describes the behavior of the absorption curve at the absorption edge. In this formula, ν is the absorption coefficient and $h\nu$ is the photon energy, E_g is the optical band gap energy, and A is the transition probability, which can be assumed to be a constant value in the considered optical frequency range. α can be calculated from the Beer-Lambert law;

$$\alpha = \frac{1}{d}\ln\frac{1}{T} \tag{2}$$

In which T is the transmittance and d is the thickness of material. Here d was taken to be 1 cm which is the size of spectroscope cuvette.

The value of m indicates the type of transition, m=1/2, 2, 3/2 or 3 for allowed direct, allowed indirect, forbidden direct and forbidden indirect electronic transitions, respectively. To calculate the bandgap of the samples, we plotted the $(\alpha h\nu)^{1/m}$ versus the photon energy $h\nu$. This graph was linear around the absorption edge and the amount the optical band gap energy of the samples was its intercept with x axis. To obtain the bandgap of each sample, a tangent line to their absorption edge was drawn and its intercept with x axis was extracted. In this study, we considered the allowed and direct transition mode (m=1/2). The Tauc diagrams in Figs. 5a and b show the bandgap of spherical and rod shaped ZnO nanostructures which were 3.75 eV and 3.07 eV respectively. The bandgap energy of nanomaterials decreases with increasing their size [24]. For the case of synthesized spherical and rod shaped ZnO nanostructures, the bandgap energy decreased with increasing their sizes. At this step we can conclude that by using laser ablation and hydrothermal methods two kinds of ZnO nanostructures

with different sizes and morphologies were synthesized successfully.

3.2 Antibacterial

Microbial or bacterial culture medium is a process that places bacteria in suitable conditions so that they find the ability to grow and reproduce. Microbes are unicellular organisms, that is, they perform all vital functions independently and without the need of another cell. Microbes need food, water and nutrients. The microbial culture environment is a completely nutritious environment that has all requirements for the growth of a bacterium. Nutrient agar culture medium is a solid medium containing all requirements for the growth of bacteria. The pH of nutrient agar at 25 °C is neutral.

To study the effects of ZnO nanostructures, we first supplemented of petri dished with *E. coli* and incubated with different forms of ZnO nanostructures. Numbers of survival colonies under the irradiation of 1 and 2 UV lamps were counted every 5 minutes. The pictures of petri dishes are presented in Figs. 6 and 7 for the case of spherical shape and nanorod ZnO nanostructures respectively and numerical results are shown in Fig. 8. Photocatalytic activities of ZnO nanostructures with spherical and nanorod morphologies are presented in Figs.8a and 8b respectively. In the presence of UV radiation, the total removal time of *E. Coli* bacteria was decreased to almost 10 minutes. Experiments began with 500 colonies. After 1 minute with 100 W (200 W) UV irradiations, for the case of spherical NPs, number of colonies was decreased to 400 (300). Number of colonies was decreased to 290 (170) after 2 minutes with 100 W (200 W) UV radiations. In 5 minutes number of colonies was decreased only to 24% (6%) under the irradiation of 100 W (200 W) UV radiations. For the nanorod ZnO nanostruc-
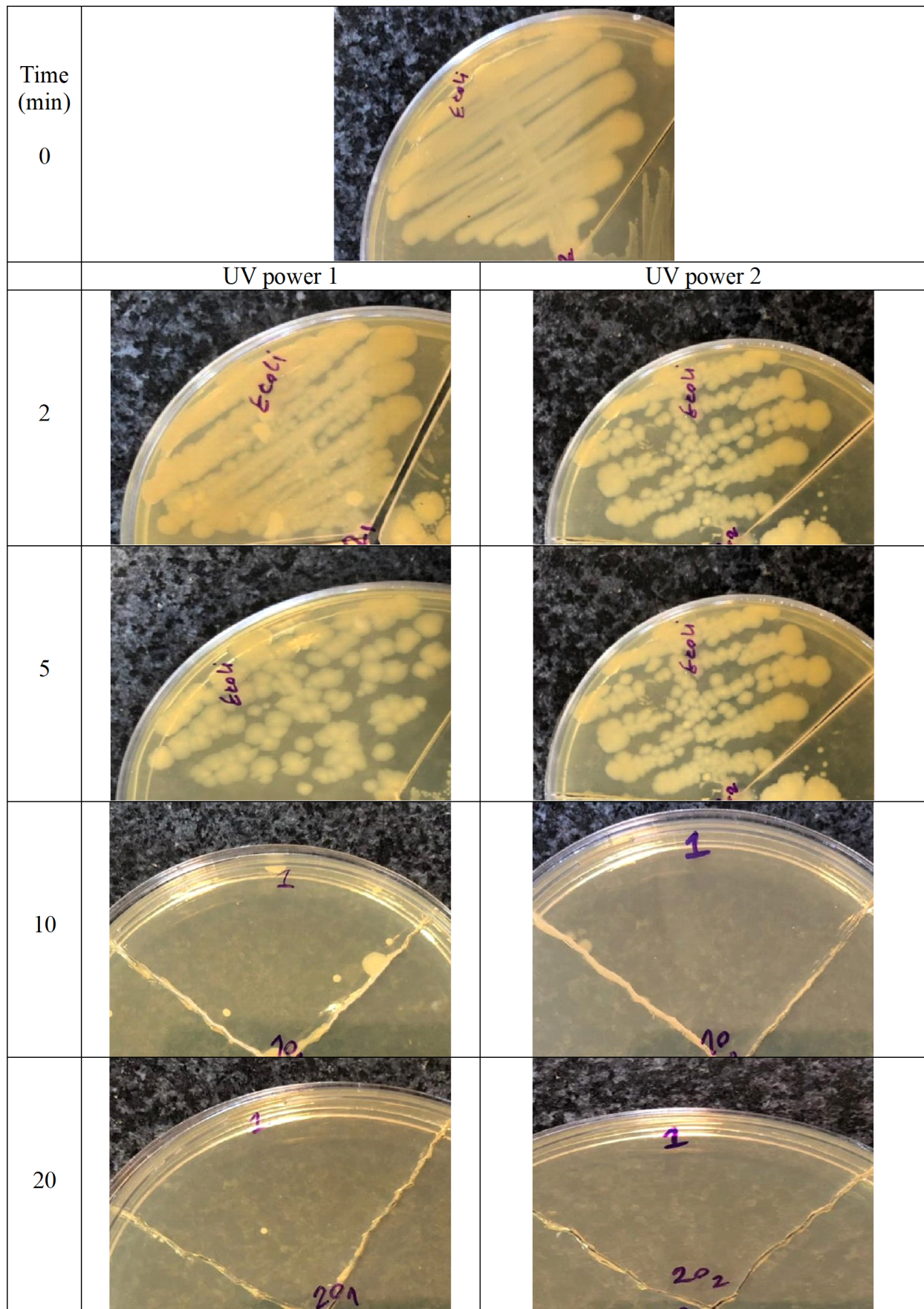
Figure 6. Antibacterial effect of spherical ZnO nanoparticles in the time interval of 0 to 20 min.
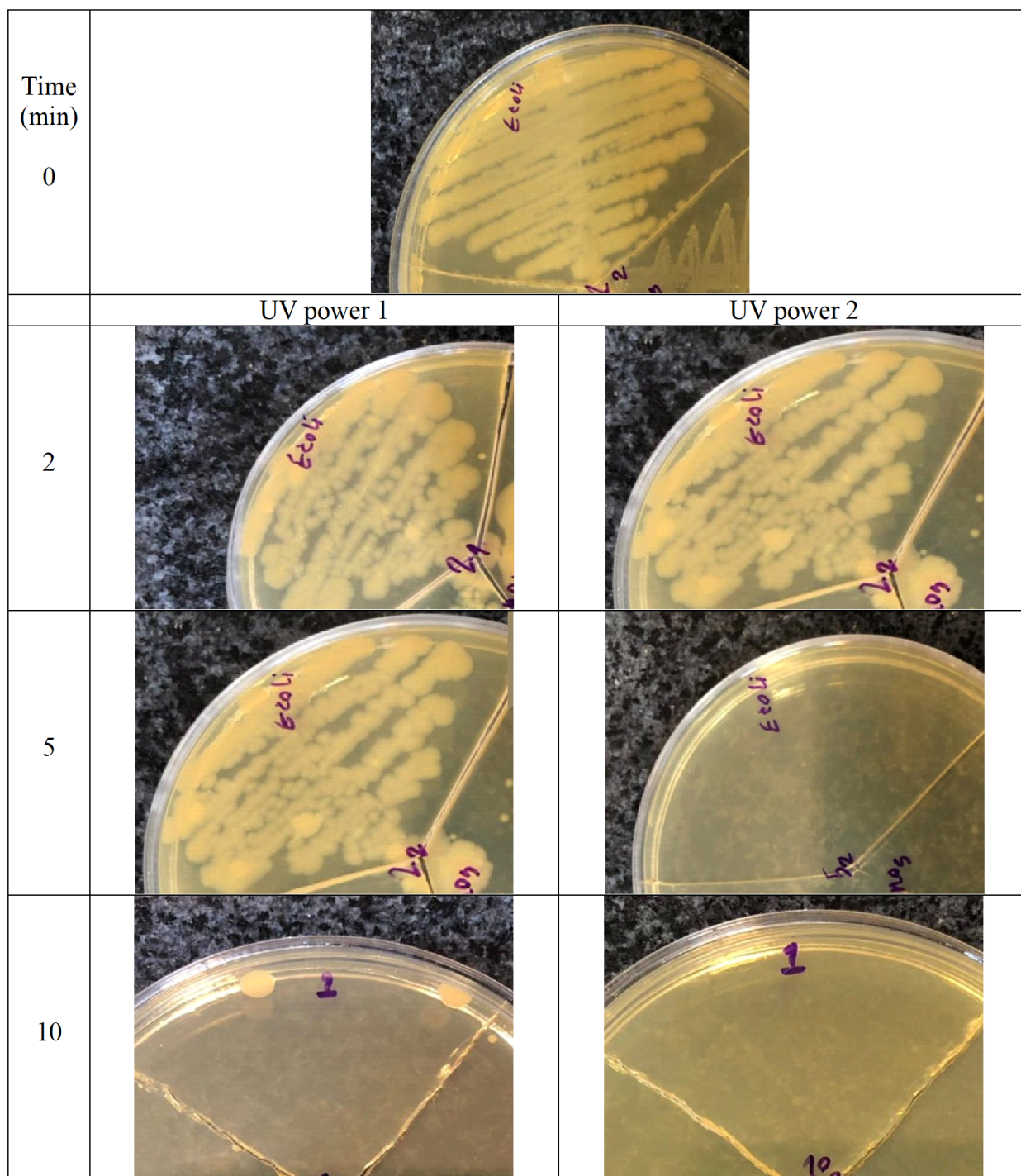
Figure 7. Antibacterial effect of nanorod ZnO nanostructures in the time interval of 0 to 10 min.

tures the same scenario was repeated with higher speed in comparison with spherical NPs. After 1 minute with 100 W (200 W) UV irradiations, number of colonies was decreased to 400 (300). After 2 minutes with 100 W (200 W) UV irradiations, number of colonies was decreased to 200 (90). Results confirm that the larger area of nanorod nanostructures are not only effective in contact with bacteria but also have positive effects in the process of UV absorption. The smaller bandgap energy of ZnO nanorods is another effective parameter in increasing its disinfection efficiency in comparison with spherical ZnO nanoparticles. In 5 minutes,

number of colonies was decreased only to 10% (4%) under the effects of 100 W (200 W) UV radiations.

Evolution of the morphology of *E. coli* cells are represented via SEM images in Figs. 9. At the original state (Fig. 9a), the cells had the full membrane with smooth surface. Figs. 9b and 9c shows the *E-coli* cells which was incubated with spherical and rod shape ZnO nanostructures after 5 minutes under the illumination of 1 UV lamp. ZnO nanostructures were appeared as the white particles in these figures. They were dispersed on the surface of nutrient agar and *E-coli* colonies. It can be seen that the membranes of all
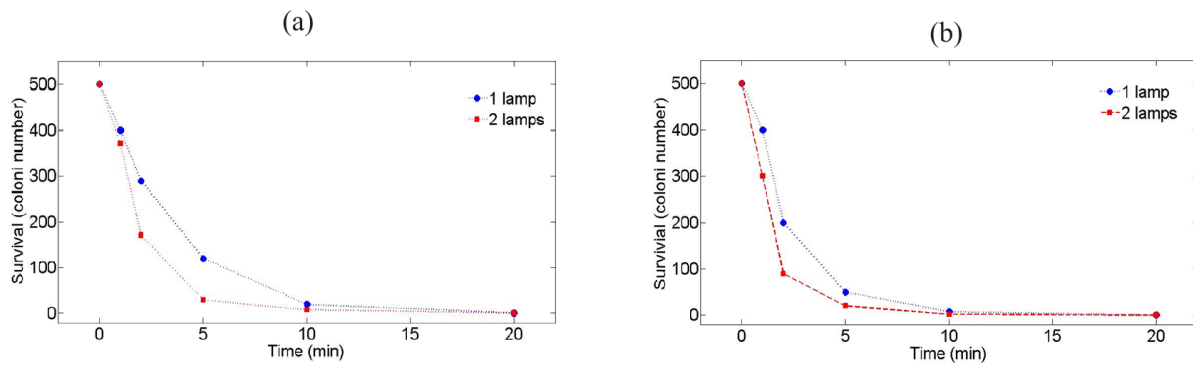
Figure 8. Effects of UV radiation intensity on photocatalytic activities of ZnO nanoparticles in inactivation of E.Coli bacteria. a) spherical shape NPs, b) nanorod NPs.
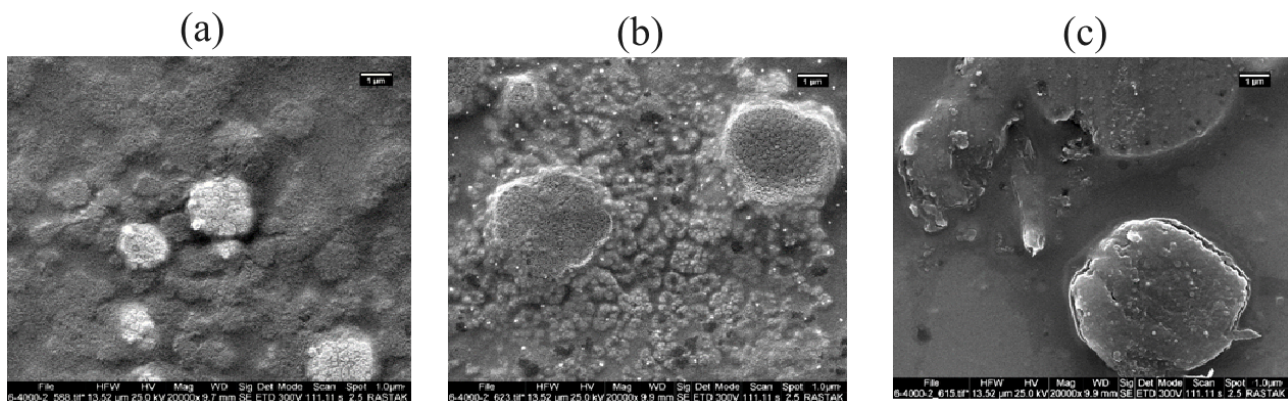

Figure 9. SEM image of untreated gram negative *Escherichia coli* bacteria (a) and the same bacteria after 5 min exposer to 1 UV lamp in the presence of spherical (b) and nanorod (c) spherical ZnO nanoparticles.

cells became indistinct and messy, and severe adhesion occurred among them. The initial antibacterial action of ZnO nanostructures against *E. coli* cells is to destruct the cell membrane which is the main organism of any cells against external attached. After the membrane distraction, the intercellular dissolved matters including proteins, and sugars flowed out gradually leaded to complete decay of the cell. Furthermore, after membrane destruction, the UV photons may find a leak to enter the cell and alter the molecules which are located inside it.

4. Conclusion

Zinc oxide nanostructures with two morphologies were synthesized by laser ablation (spherical shape) and hydrothermal (rod-shape) methods and their photocatalytic activities against *Escherichia coli* bacteria were investigated. Beside morphology, effects of size, time, and UV radiation were also studied. In this experimental condition, in any case, including both morphologies of ZnO nanostructures, with or without UV irradiation, after about 20 minutes the water medium was disinfected completely. To observe the effects of different parameters, the disinfection percentages were extracted from the presented data in the first 5 minutes

Table 1. The percentage of the results of photocatalytic activities of water disinfection of Escherichia coli by two ZnO morphologies in the first 5 minutes of deactivation process.

Morphology	Dark condition (%)	1 UV lamp (%)	2 UV lamps (%)
Spherical	40	76	94
Nanorod	50	90	96

of inactivation process. Results are presented in Table 1. There is 10% difference between the disinfection efficiency of rod shaped and spherical ZnO nanostructures in the absence of UV radiation. In this case we observe the effect of contact area of nanostructures with bacteria. In the case of 1 UV lamp radiation the difference between the disinfection efficiency increases to 14%. Here we have 3 important parameters which increases the disinfection efficiency. All of them depends on the main parameter which is area of nanostructures. Increasing the size of nanostructure increases the contact area, UV effective absorption surface, and also decreases the bandgap energy of nanostructures. With increasing the intensity of UV radiation these differences can be compensated and both ZnO nanostructures disinfection efficiencies become almost equal.

Authors Contributions
Design and setup of the experiments as well as acquisition of data were done by Sekineh Khodadad. She also contributed in analysing the data and writing the draft of the paper. Davoud Dorranian was the supervisor of the project. Conception and design of the setup, data analysing, and finalizing the paper were carried out by him. All experiments were accomplished in Reza Mirnejad's Laboratory. Experimental setup, data acquisition, and part of data analysing was completed by him. Peyman Azimi Anaraki and Tania Davari Mahabadi were contributed in analysing the data and writing the draft of the paper.

Availability of Data and Materials
The data that support the findings of this study are available from the corresponding author, upon reasonable request.

Conflict of Interests
The authors declare that they have no known competing financial interests or personal relationships that could have appeared to influence the work reported in this paper.

References

[1] M. Irannezhad, B. Ahmadi, J. Liu, and D. Chen. "Global water security: A shining star in the dark sky of achieving the sustainable development goals". *Sustainable Horizons*, **1**:100005, 2022.

[2] D. G. Larsson and C. F. Flach. "Antibiotic resistance in the environment". *Nature Reviews Microbiology*, **20**:257, 2022.

[3] S. V. Gudkov, D. E. Burmistrov, D. A. Serov, M. B. Rebezov. A. A. Semenova, and A. B. "Lisitsyn; A mini review of antibacterial properties of ZnO nanoparticles". *Frontiers in Physics*, **9**:1, 2021.

[4] M. Yasuyuki, K. Kunihiro, S. Kurissery, N. Kanavillil, Y. Sato, and Y. Kikuchi. "Antibacterial properties of nine pure metals: a laboratory study using Staphylococcus aureus and Escherichia coli". *Biofouling*, **26**: 851–858, 2010.

[5] J. A. Lemire, J. J. Harrison, and R. J. Turner. "Antimicrobial activity of metals: mechanisms, molecular targets and applications". *Nat. Rev. Microbiol*, **11**: 371–384, 2013.

[6] R. Turner. "Metal-based antimicrobial strategies". *Microb Biotechnol*, **10**:1062–1065, 2017.

[7] E. R. Stadtman. "Oxidation of free amino acids and amino acid residues in proteins by radiolysis and by metal-catalyzed reactions". *Annual Rev. Biochem*, **62**: 797–821, 1993.

[8] E. R. Stadtman. "Levine RL free radical-mediated oxidation of free amino acids and amino acid residues in proteins". *Amino Acids*, **25**:207–218, 2023.

[9] K. W. Guo. "Property of zinc oxide (ZnO) nanostructures potential for biomedical system and its common growth mechanism". *J. Appl. Biotechnol. Bioeng*, **2**: 197–202, 2017.

[10] M. Heinlaan, A. Ivask, I. Blinova, H. C. Dubourguier, and A. Kahru. "Toxicity Of nanosized and bulk ZnO, CuO, and TiO2 to bacteria vibrio fischeri and crustaceans daphnia magna and thamnocephalus platyurus". *Chemosphere*, **71**:1308–1316, 2008.

[11] L. Zhang, Y. Jiang, Y. Ding, N. Daskalakis, L. Jeuken, and M. Povey. "Mechanistic investigation into antibacterial behavior of suspensions of ZnO nanoparticles against E. Coli". *J. Nanoparticle Res*, **12**:1625–1636, 2010.

[12] M. Ketabchi, Kh. Iessazadeh, and A. Massiha. "Evaluate the inhibitory activity of ZnO nanoparticles against standard strains and isolates of Staphylococcus aureus and Escherichia coli isolated from food samples". *JFM*, **4**:63–74, 2017.

[13] J. Sawai and T. Yoshikawa. "Quantitative evaluation of antifungal activity of metallic oxide powders (MgO, CaO and ZnO) by an indirect conductimetric assay". *J. Appl. Microbiol*, **96**:803–809, 2004.

[14] S. Thakur and S. K. Mandal. "enhanced photocatalytic activity and antibacterial action against Escherichia coli". *New J. Chem*, **27**:11796–11807, 2020.

[15] N. B. Raj, N. T. PavithraGowda, O.S. Pooja, B. Purushotham, M. R. Anil Kumar, S. K. Sukrutha, C. R. Ravikumar, H. P. Nagaswarupa, H. C. Ananda Murthy, and S. B. Boppana. "Harnessing ZnO nanoparticles for antimicrobial and photocatalytic activities". *J. Photochem. Photobiology*, **6**:100021, 2021.

[16] S. Thakur, S. Neogi, and A. K. Ray. "Morphology-controlled synthesis of ZnO nanostructures for caffeine degradation and Escherichia coli inactivation in water". *Catalysts*, **11**:63, 2021.

[17] S. Sharma, K. Kumar, N. Thakur, S. Chauhan, and M. S. Chauhan. "The effect of shape and size of ZnO nanoparticles on their antimicrobial and photocatalytic activities: a green approach". *Bullet. Mater. Sci*, **43**: 20, 2020.

[18] J. Sawai. "Quantitative evaluation of antibacterial activities of metallic oxide powders (ZnO, MgO and CaO) by conductimetric assay". *J. Microbiological Meth*, **54**:177–182, 2003.

[19] G. R. Navale, M. Thripuranthaka, D. J. Late, and S. S. Shinde. "Antimicrobial activity of ZnO nanoparticles against pathogenic bacteria and fungi". *JSM Nanotechnol. Nanomed*, **3**:1033–1035, 2015.

[20] N. Jones, B. Ray, R. T. Koodali, and A. C. Manna. "Antibacterial activity of ZnO nanoparticles suspensions on a broad spectrum of microorganisms". *FEMS Microbiol Lett*, **279**:71–76, 2008.

[21] C. Hallmich and R. Gehr. "Effect of pre- and post-UV disinfection conditions on photoreactivation of fecal coliforms in wastewater effluents". *Water Res*, **44**: 2885–2893, 2010.

[22] J. C. Chang, S. F. Ossoff, D. C. Lobe, M. H. Dorfman, C. M. Dumais, R. G. Qualls, and J. D. Johnson. "UV inactivation of pathogenic and indicator microorganisms". *Appl. Environ. Microbiol*, **49**:1361–1365, 1985.

[23] D. Dorranian, E. Solati, and L. Dejam. " Photoluminescence of ZnO nanoparticles generated by laser ablation in deionized water ". *Applied Physics A*, **109**: 307–314, 2012.

[24] E. Solati, L. Dejam, and D. Dorranian. "Effect of laser pulse energy and wavelength on the structure, morphology and optical properties of ZnO nanoparticles". *Opt. Laser Technol*, **58**:26–32, 2014.

[25] M. Moradi, E. Solati, S. Darvishi, and D. Dorranian. "Effect of aqueous ablation environment on the characteristics of ZnO nanoparticles produced by laser ablation". *J. Cluster Sci*, **27**:127–138, 2016.

[26] S. Mohan, M. Vellakkat, A. Aravind, and U. Reka. "Hydrothermal synthesis and characterization of zinc oxide nanoparticles of various shapes under different reaction conditions". *Nano Express*, **1**:030028, 2020.

[27] P. Mosayebi, D. Dorranian, and K. Behzad. "Investigating the implementation of ZnO nanoparticles as a tunable UV detector for different skin types". *Surface Review and Letters*, **25**:1850062, 2018.

[28] CLSI. "Methods for antimicrobial dilution and disk susceptibility of infrequently isolated or fastidious bacteria, approved guideline, CLSI document M45-A2". *Clinical and Laboratory Standards Institute Wayne, Pennsylvania 19087, USA*, , 2010.

[29] J. Amani, K. A. Barjini, M. M. Moghaddam, and A. Asadi. "In vitro synergistic effect of the CM11 antimicrobial peptide in combination with common antibiotics against clinical isolates of six species of multidrug-resistant pathogenic bacteria". *Protein Peptide Lett*, **22**:940–951, 2015.

[30] H. Moravej, M. Fasihi-Ramandi, M. M. Moghaddam, and R. Mirnejad. "Cytotoxicity and antibacterial effect of Trp-substituted CM11 cationic peptide against drug-resistant isolates of Brucella melitensis alone and in combination with recommended antibiotics". *Int. J. Peptide Res. Therapeut*, **25**:235–245, 2019.

[31] J. Tauc. "Optical properties and electronic structure of amorphous Ge and Si". *Materials Research Bulletin*, **3**:37–46, 1968.